International Journal of Biological Macromolecules 217 (2022) 562–571

Contents lists available at ScienceDirect

International Journal of Biological Macromolecules

journal homepage: www.elsevier.com/locate/ijbiomac

Poly(L-lactic acid)/poly(ethylene oxide) based composite electrospun fibers loaded with magnesium-aluminum layered double hydroxide nanoparticles☆

Esra Altay Ozturk [a], Zeynep Ruya Ege [b,c], Semiha Murat [d], Gokce Erdemir [e,i,j], Serap Kuruca [e], Ziya Engin Erkmen [f], Ozgur Duygulu [g], Oguzhan Gunduz [b,c], Tuncer Caykara [a], Mehmet S. Eroglu [b,h,*]

[a] Department of Chemistry, Faculty of Science, Gazi University, Besevler, 06500 Ankara, Turkey
[b] Department of Materials Science and Engineering, Technology Faculty, Marmara University, Aydınevler, Maltepe, 34854, Istanbul, Turkey
[c] Center for Nanotechnology & Biomaterials Application and Research at Marmara University, Aydınevler, Maltepe, 34854 Istanbul, Turkey
[d] Yildiz Technical University, Chemical Engineering Department, Davutpasa, 34210 Istanbul, Turkey
[e] Department of Physiology, Faculty of Medicine, Istanbul University, Istanbul 34390, Turkey
[f] Metallurgical and Materials Engineering Dept., Faculty of Engineering, Marmara University, Aydınevler, Maltepe, 34854, Istanbul, Turkey
[g] TUBITAK Marmara Research Center Materials Institute, Gebze, Kocaeli, Turkey
[h] TUBITAK-UME, Chemistry Group Laboratories, PO Box 74, 41470, Gebze, Kocaeli, Turkey
[i] Department of Molecular Medicine, Aziz Sancar Institute of Experimental Medicine, Istanbul University, Istanbul 34390, Turkey
[j] Molecular Cancer Research Center (ISUMKAM), Istinye University, Istanbul 34010, Turkey

ARTICLE INFO

Keywords:
PLA/PEO electrospun mat
Mg-Al LDH
PLA

ABSTRACT

Two types of Mg—Al layered double hydroxide nanoparticles, Mg—Al LDH, at Mg:Al ratio of 2:1 and 3:1were prepared and used as inorganic fillers to improve the mechanical properties of poly(lactic acid)/poly(ethylene oxide) (PLA/PEO) electrospun composite fibers. Their detailed structural characterization was performed using X-ray diffraction (XRD) and transmission electron spectroscopy (TEM) techniques. Spectroscopic, thermal, mechanical, and morphological properties of the electrospun composite fibers, and cell proliferation on their surface, were examined. XRD and TEM analyses showed that the LDH nanoparticles were 50 nm in size and the Mg:Al ratio did not affect the average spacing between crystal layers. Fourier transform infrared (FTIR) and thermal analyses (TA) revealed the compatibility of the filler and the polymer matrix. The nanoparticles considerably improved the mechanical properties of the electrospun mats. The tensile strength and elongation at break values of the composite samples increased from 0.22 MPA to 0.40 MPa and 12.2 % to 45.66 %, respectively, resulting from the interaction between LDH and the polymer matrix. Scanning electron microscopy (SEM) and MTT analyses demonstrated that the electrospun composite fibers supported the SaOS-2 cells attachment and proliferation on the fiber surfaces, along with their suitable cytocompatibility.

1. Introduction

Biocompatible and biodegradable polymers are emerging materials for a wide range of applications in environmental and medical issues [1]. Among the biodegradable polymers, poly(lactic acid) (PLA) is one of the most promising linear thermoplastic polyester. This polymer is mainly produced by natural materials fermentation such as corn, starch, sugarcane, etc., while partially produced by lactide and lactic acid polymerization [2]. PLA has been widely studied in various applications including food packaging [3], textile fibers, surgery sutures, and biomedicine such as stent and dialysis membrane preparations [4], tissue engineering, wound dressing, and drug delivery [5]. Despite favorable thermal, biological, and physical properties like easy processability, non-toxicity, high tensile strength, and satisfactory biodegradability,

☆ This publication is dedicated to late Professor Tuncer Caykara

* Corresponding author at: Department of Materials Science and Engineering, Technology Faculty, Marmara University, Aydınevler, Maltepe, 34854 Istanbul, Turkey.
E-mail address: mehmet.eroglu@marmara.edu.tr (M.S. Eroglu).

https://doi.org/10.1016/j.ijbiomac.2022.07.055
Received 14 April 2022; Received in revised form 3 July 2022; Accepted 8 July 2022
Available online 15 July 2022

PLA has low flexibility, low crystallinity, and inadequate barrier properties [2]. Preparation of copolymers and blends of PLA with biocompatible polymers, and nanocomposite formulations with suitable nano-sized fillers partly overcome these drawbacks. PLA blends with a variety of polymers including poly-ε-caprolactone [6], starch [7], poly (ethylene glycol) (PEG) [8], and poly(ethylene oxide)(PEO) [9,10] were reported.

PEO is a non-ionic and non-toxic high molecular weight linear polyether, which is highly soluble in aqueous media and organic solvents. As it has an excellent hemocompatibility and easy processability, PEO has been an essential polymer for surface and bulk modification of natural polymers [11,12], drug delivery systems, and hemodialysis membranes [13]. PEO was approved by FDA for clinical use. Its ethylene oxide repeating groups are capable of making hydrogen bonding via hydrophilic etheric oxygen bridge with primary hydroxyl groups of glycosides and their derivatives [11]. Because of the flexibility and hydrogen bonding capability, PEO improves the mechanical properties of its blends with rigid biodegradable polymers. At relatively higher concentrations, the PEO matrix tends to crystallize in blend films and causes phase segregation. In our previous studies, we reported the suppressed crystallinity of PEO in blend films, prepared with chitosan and sodium alginate, which provided a more amorphous and homogeneous morphological structure, leading to a more flexible and biocompatible material [11,12]. Nijenhuis et al. studied PLA compatibility of high molecular weight PEO and reported a decreased equilibrium melting temperature and increased flexibility with increased PEO portion. This finding could be a proof of the intermolecular interactions and, thus, compatibility of the polymers [10,14]. They studied the melt crystallization of PLA-PEO blends under various conditions and reported that the glass transition temperature (Tg) of PEO increased with increasing PLA content.

Layered double hydroxides-based fillers have been attracting increasing attention to improve the thermal, mechanical, and barrier properties of PLA [15,16]. Generally, LDHs are a class of anionic clays, having a stacked-layer structure with a general formula of $[M^{II}_{1-x}M^{III}_{x}(OH)_{2x}]^{x+}(A^{n-})_{x/n}.mH_2O$ [16–18], where M^{II} and M^{III} are di- and trivalent metal cations, respectively, occupying octahedral sites in a brucite-like layer, and A^{n-} represents anions (i.e. NO_3^- and $CO_3^{=}$) located in the hydrated interlayer gallery. With respect to the general formula, depending on the stoichiometric coefficient (x), the change in the amount of di- and trivalent cations and interlayer anion provides a large class of isostructural materials. Therefore, tunable anionic exchange capacity makes the LDHs commercially versatile materials for drug carriers in nanomedicine, anion exchanger, catalyst support, pharmaceuticals, and agriculture [19]. Among the LDHs, due to the endocytosis property, Mg—Al layered double hydroxide (Mg—Al LDH) is a biocompatible material and a versatile drug carrier in anionic form. Depending on the particle size and shape, this material is of particular interest in the targeting delivery of anticancer drugs and biomolecules [19].

Electrospinning is a method used to produce ultrafine fibers ranging from micro to nanometer diameters. In the electrospinning process, a polymer solution is transferred to the needle tip, and then the polymer solution becomes a droplet at the tip of the needle. An electric field is applied, and nanofiber is formed on the metal plate. The ultrafine fibers can be obtained from different materials such as synthetic and natural polymers, polymer blends, and polymers loaded with nanoparticles or active agents [20,21]. Electrospun nanofibers are highly preferred in biomedical applications such as tissue engineering scaffolds, wound healing materials, drug delivery, filtration, affinity membrane, enzyme immobilization, small diameter vascular graft implants, healthcare, biotechnology, and environmental engineering [22].

Herein, preparation and characterization of PLA/PEO-based electrospun nano/micro composite fibers filled with Mg—Al LDH nanoparticles are reported. Their spectroscopic, thermal, mechanical, morphological, and biological characterizations were performed. Many articles on LDH-filled PLA or PEO nanocomposite films [15,16,23–25] and PLA/PEO blends [10,20,26,27] are available in the literature. However, to our knowledge, there is no report on the PLA/PEO-based composite electrospun fibers filled with Mg—Al LDH nanoparticles. In the case of severe bone injury, electrospun bandages prepared from biodegradable polymers have been widely used to promote osteoinduction and bone regeneration. These type of materials provide a cell scaffold for human osteoblast cells. Mechanical properties and cell proliferation on their surface are important factors. Mg/Al LDH nanofiller could augment cell proliferation and mechanical properties of such electrospun fibers. In addition to cell scaffolds, they may have remarkable potential for membrane separation of biological molecules, tissue engineering, and implant materials.

2. Materials and methods

2.1. Materials

Poly (L-lactic acid) (PLA) (Natureplast PLE 005) from vegetable resources, was supplied from Nature Plast., France, with a density of 1.25 g/cm^3 and a melting temperature in the range of 145–155 °C [28]. Polyethylene oxide (PEO 300.000) was purchased from Sigma-Aldrich and used as received. Aluminum nitrate-9-hydrate ($Al(NO_3)_3.9H_2O$) and magnesium nitrate hexahydrate ($Mg(NO_3)_2.6H_2O$) were used for co-precipitation of Mg—Al LDH in aqueous media. Sodium hydroxide and sodium carbonate were used for adjusting the pH for precipitation, and chloroform was used as a solvent for electrospun compositions. They were supplied from Sigma Aldrich and used as received.

2.2. Preparation of Mg—Al LDH nanoparticles

Magnesium-Aluminum layered double hydroxide (Mg—Al LDH) nanoparticles at two Mg:Al ratios of 2:1 and 3:1 (mol/mol) with the formulas of $Mg_4Al_2(CO_3)(OH)_{12}{\cdot}4H_2O$ and $Mg_6Al_2(CO_3)(OH)_{16}{\cdot}4H_2O$, respectively, were successfully synthesized according to our previous study [23]. Regarding the synthesis of Mg—Al LDH having Mg:Al ratio of 3:1, known as hydrotalcite, an aqueous solution of $Mg(NO_3)_2.6H_2O$ (75 mmol) and $Al(NO_3)_3.9H_2O$ (25 mmol) (100 mL) was added into a mixture of Na_2CO_3 (0.025 mol) and NaOH (0.2 mol) dissolved in water (100 mL). The slurry product was vigorously stirred at a constant speed for 12 h at 65 °C, and the pH was adjusted to 9.0–9.5 with 1.0 M NaOH solution. The precipitate was filtered, washed with distilled water, and dried at 70 °C under vacuum [18]. Detailed transmission electron microscopy (TEM) and X-ray diffraction spectroscopy (XRD) characterizations of the nanoparticles were performed.

2.3. Preparation and characterization of electrospun solutions

The electrospun compositions are collected in Table 1. Sample S-1 was prepared as a control at a PLA/PEO ratio of 8/5 in chloroform, without including Mg—Al LDH nanoparticles. For the samples S-2, S-3, S-4, and S-5, stock solutions of Mg—Al LDH 2:1 and 3:1 at 1 % and 2 % ratios in chloroform were prepared and mixed with the desired amount of PLA and PEO. They were stirred at room temperatures for 24 h to obtain homogeneous clear electrospun solutions. The physicochemical properties of the electrospun solutions i.e., viscosity (DV-E, Brookfield AMETEK, USA), density (by using a 10 mL particular gravity flask), electrical conductivity (a conductivity meter Cond 3110 SET 1, WTW, Germany), and surface tension (Sigma 703D, Attension, Germany) were determined at 25 °C (Table 1).

2.4. Production of the micro/nano-composite electrospun fibers

Electrospinning was performed using an electrospinning unit NS24, Inovenso Co., at room temperature. Polymer solutions were filled into a 10 ml syringe, which was attached to an 18-gauge needle in the

Table 1
Compositions and physico-chemical properties of the electrospun solutions at 25 °C[a].

Sample no	Concentration of the electrospun solution in chloroform (*w/v*)	Surface tension (mN/m)	Electrical Conductivity (μS/Cm)	Viscosity (Pa.s)	Density (kg/m^3)
S-1	8 wt% PLA, 5 wt % PEO	29.53 ± 0.66	0.9 ± 0.1	410.21 ± 0.42	1467 ± 0.5
S-2	8 wt% PLA, 5 wt % PEO, 1wt% LDH(Mg/Al 2:1)	29.33 ± 0.53	2.3 ± 0.05	235.44 ± 0.75	1468 ± 1.2
S-3	8 wt% PLA, 5 wt % PEO, 1wt% LDH(Mg/Al 3:1)	28.35 ± 0.21	2.7 ± 0.1	343.73 ± 0.23	1487 ± 0.8
S-4	8 wt% PLA, 5 wt % PEO, 2wt% LDH(Mg/Al 2:1)	28.29 ± 0.70	2.4 ± 0.2	197.56 ± 0.88	1471 ± 0.3
S-5	8 wt% PLA, 5 wt % PEO, 2wt% LDH(Mg/Al 3:1)	28.29 ± 0.70	2.4 ± 0.2	197.56 ± 0.88	1471 ± 0.3

[a] The remaining part in the electrospun formulations is chloroform used as solvent.

electrospinning system. The flow rate of the system was kept at 3 mL/h using a syringe pump (NE-300, New Era Pump Systems, Inc., USA) and the distance between the needle and the collector plate was adjusted to 150 mm. After determining the system flow rate and experimental distance, attempts were made to determine the appropriate voltage for fiber formation and the best composite fiber was produced when 16 kV voltage was applied between the syringe and the collector. For all electrospun solutions, 3 mL/h flow rate, 150 mm distance, and 16 kV voltage electrospinning process were applied at room temperature.

2.5. Fourier transform infrared spectroscopy (FTIR)

FTIR spectra of the nanocomposite fibers were recorded using Jasco FT/IR 4700 spectrometer having the software of OPUS Viewer (version 6.5). Measurements were conducted between 400 and 4000 cm^{-1} in transmission mode.

2.6. Differential scanning calorimetry (DSC)

Melting temperatures of the PLA and PEO in composite fibers were determined using Perkin Elmer Jade DSC (PerkinElmer Inc., Mass., USA) and the data were evaluated using Pyris software. DSC was calibrated according to indium melting point and melting enthalpy. All the samples were tested in a crimped aluminum pan under a dynamic Ar atmosphere (200 ml/min) at 10 °C/min heating rate. Melting points of PLA and PEO were obtained as the peak values of melting endotherms.

2.7. Thermal gravimetric analysis (TGA)

Dynamic weight loss (TGA) and derivative weight loss (DTGA) curves of the samples were recorded on a Seiko-EXSTARTG/DTA7300 model thermal analysis system. All the tests were performed under a dynamic Ar atmosphere (200 ml/min) at a heating rate of 10 °C/min with 5–7 mg samples. Data were evaluated using Muse software.

2.8. X-ray diffraction (XRD) analysis

Morphology of the Mg—Al LDH nanoparticles was studied using an X-ray diffractometer (RIGAKU®D/MAX2200/PC). Each sample (12 mm × 12 mm) was placed on a special amorphous glass, and then X-ray diffraction patterns were recorded. Analyses were performed at 40 kV and 30 mA with CuKα radiation ($\lambda_{K\alpha} = 1.541$ Å) over a 2θ range between 5° and 60° at a scan speed of 2°/min. OriginPro 7.0 software (OriginLab Corporation, MA, USA) was used to convert the obtained data to diffractograms (XRD) and they were evaluated.

2.9. Scanning Electron microscopy (SEM)

The size and morphology of the electrospun fibers and cell proliferation on their surface were examined using scanning electron microscopy (Hitachi VP-SEM S-3400 N). Before the analyses, the surfaces of the samples were sputter-coated with gold, and the images were obtained at 5 eV accelerating voltage at different magnifications. The average diameter and size distribution of the micro/nanofibers were determined from the thickness of randomly selected 100 fibers on SEM images. The image data were evaluated using image software (ImageJ, Brocken Symmetry software). For the SEM analyses of the cell proliferation, micro/nanofibers were cultured and SaOS-2 cells were seeded on their surface. After 24 h of incubation, images were obtained at 5.0 kV acceleration voltage at different magnifications.

2.10. Transmission electron microscopy (TEM)

Transmission Electron Microscopy studies (TEM) were performed on JEOL JEM 2100 HRTEM at 200 kV. Images were recorded by Gatan Model 833 Orius SC200D CCD Camera. Carbon support film-coated copper TEM grids (Electron Microscopy Sciences, CF200-Cu, 200 mesh) were used.

2.11. Tensile test

Stress-strain behavior of the electrospun mats was recorded on an Instron 4411 tensile tester at room temperature with a crosshead speed of 5 mm/min. The initial data was evaluated by Bluehill 2 software (Elancourt, France). The thickness of each sample was measured using a digital micrometer (Mitutoyo MTI Corp., USA). The test results were considered in context with the ultimate strength and ultimate elongation values, which were average values of six measurements and expressed in MPa and percentage elongation, respectively (Table 2).

2.12. Cytotoxicity study

The SaOS-2 human bone osteosarcoma cell line was obtained from American Type Culture Collection (ATCC). Cells were cultured in Dulbecco's modified Eagle medium (DMEM, Gibco) with 10 % Fetal bovine serum (FBS, Gibco) and 1 % penicillin/streptomycin in a 5 % CO_2 humidified air incubator, maintained at 37 °C. When the cells reached 80 % of confluence, they were washed with PBS and trypsinized with 0.25 % Trypsin-EDTA for passaging and seeding each time. The confluent cells were used in cytotoxicity tests and SEM investigations.

Initially, the conditioned medium was prepared to understand any possible toxic effect induced by possible ionic leach-out product from the samples into the medium. Fresh medium (3 mL) was added into tubes with a piece (~0,05 g) of electrospun fibers, which were kept in the incubator. After 3 days, the conditioned medium was extracted and used in cytotoxicity tests. 3-{4,5-dimethylthiazol-2yl}-2,5-diphenyl-2*H*-tetrazolium bromide (MTT) assays were performed in 96-well plates. The SaOS-2 cells (about 10^5cells per well) were seeded onto the 4 h UV sterilized polymers and incubated for 3 days. Cell viability was measured by determining mitochondrial NADH/NADHP–dependent dehydrogenase activity, which resulted in the cellular conversion of 3-(4, 5-dimethylthiazol-2-gl)-5-(3-carboxy methoxyphenyl)-2-(4-sulfophenyl-2H) tetrazolium salt into a soluble formazan dye. After 3 days, supernatants were removed, and 10 μl MTT(5 mg/ml- Sigma) solution was added to each well. Following incubation at 37 °C for 3.5 h and being kept in dark in a humidified atmosphere at 5 % CO_2 in the air, MTT was received by active cells and reduced in mitochondria to an insoluble purple formazan granule [29]. Subsequently, the supernatant was discarded, and the precipitated formazan was dissolved in dimethyl

Table 2
The compositions of the micro/nanocomposite PLA/PEO mats and their tensile test results[a].

Sample no	PLA (wt %)	PEO (wt %)	Mg/Al LDH (2:1) (wt%)	Mg/Al LDH (3:1) (wt%)	UltimateTensile strength (Mpa)	Ultimate Elongation (%)
S-1	61.50	38.5	–	–	0.22 ± 0.016	12.210 ± 2.189
S-2	60.88	38.5	0.62	–	0.19 ± 0.077	12.708 ± 0.518
S-3	60.88	38.5	–	0.62	0.19 ± 0.038	13.849 ± 5.641
S-4	60.26	38.5	1.24	–	0.32 ± 0.039	43.135 ± 8.158
S-5	60.26	38.5	–	1.24	0.40 ± 0.043	45.662 ± 0.165

[a] Compositions were calculated from the data in Table 1.

sulfoxide (100 μL per well). The optical density of the solution was evaluated using a microplate spectrophotometer (Kayto RT-2100C) at a wavelength of 570 nm. For the cell proliferation study, the electrospun fibers were placed into the wells of 6-well cell culture plates and sterilized for 4 h. The SaOS-2 cells were seeded in these plastic dishes and incubated for 24 h in a humidified incubator at 37 °C with 95 % air and 5 % CO_2. After 24 h, the media was removed, and the specimens were fixed with a 3 % volume fraction of glutaraldehyde, subjected to graded (30–100 %) alcohol dehydration, kept at −20 °C, SEM images of which were recorded at different magnifications.

3. Results and discussion

3.1. Physico-chemical parameters of electrospun solutions

Surface tension, electrical conductivity, viscosity, and density values of the compositions are given in Table 1. These parameters significantly affected the shape and thickness of the nanofibers during the electrospinning process [30,31]. Although the presence of Mg—Al LDH did not significantly affect the surface tension and density of the formulations, it affected the viscosity and the conductivity. An increase in electrical conductivity and a decrease in viscosity were observed with the increasing Mg—Al LDH content. Different experiments were conducted to examine the effect of the Mg—Al LDH portion of the compositions on the shape and thickness of the fibers. A decrease in the viscosity and the lowering of the surface tension at the Mg—Al LDH concentrations of 1 % and 2 % supported the formation of bead-free and uniform fibers [32,33]. According to the literature report, the viscosity and electrical conductivity of the electrospun solutions could control the fiber diameter [34]. Moreover, the effect of electrical conductivity is much higher than that of viscosity [35,36]. The higher electrical conductivity led to a decrease in fiber diameters [36].

3.2. FTIR

In a blended system, depending on the magnitude of the intermolecular interactions, the change in the IR absorption frequencies and shape of some specific peaks of the components are considered as evidence of the energetic interactions and therefore miscibility of the ingredients. The FTIR spectra of pure PLA, pure PEO, and unfilled (sample S-1) and Mg—Al LDH filled samples (S-2, S-3, S-4, and S-5) are shown in Fig. 1. The characteristic absorption bands of PEO are CH_2 stretching at 2882 cm^{-1}, C-O-C stretching vibration at 1148, 1101,1062, and 958 cm^{-1}, C—H bending absorption at 1467 cm^{-1}, and C—H wagging vibration of CH_2 groups at 1358 and 1340 cm^{-1} (Fig. 1-a). The absorption bands at 1340 and 1358 cm^{-1} are due to the wagging vibrations of CH_2 groups of PEO in the crystalline phase (Fig. 1-a) [37]. The characteristic peaks of PLA are C═O vibration peak at 1756 cm^{-1}, CH_3 asymmetrical scissoring at 1454 cm^{-1}, C—O asymmetrical stretching at 1180 cm^{-1}, C–CH_3 stretching at 1045 cm^{-1}, and C–COO stretching at 868 cm^{-1}(Fig. 1-b).

Intermolecular interaction between PEO, PLA, and the filler was evidenced by the change in shape and intensities of the CH_2 wagging absorption of PEO in the crystalline phase, which were observed at 1340 and 1358 cm^{-1} (marked in Fig. 1a). As the percentage of Mg—Al LDH increased from 0.62 to 1.24, the intensities of the characteristic peaks showed a tendency of partially merging into a single absorption peak, belonging to the CH_2 wagging absorption in the amorphous phase. This change in the IR spectrum of PEO indicated the incorporation of the filler into the PEO crystal lattice and energetic interaction with PLA [12,37]. Hydrogen bonding between -OH groups of Mg—Al LDH, C═O groups of PLA, and C-O-C etheric bridge of PEO affected the morphology of the polymer matrix, resulting in more amorphous and flexible electrospun fibers. This result was confirmed by DSC and stress-strain test.

3.3. SEM

Scanning electron microscopy (SEM) is a helpful technique for analyzing the shape and size distribution of the electrospun fibers and inorganic particles. Fig. 2a shows the SEM image and diameter distribution of unfilled PLA/PEO electrospun fibers (Sample S-1, Table 2). The homogeneous and smoothly oriented fibers, without visible beads, revealed the compatibility of the components and there was no phase segregation in the electrospun solution. The average diameter was 1913 nm (Std. dev. 720) with a large distribution of fiber size. Figs. 2b-e show SEM images of the composite samples with their diameter and size distributions. Smooth and homogeneous fiber surfaces were obtained for composite samples as well. However, the composite samples tend to

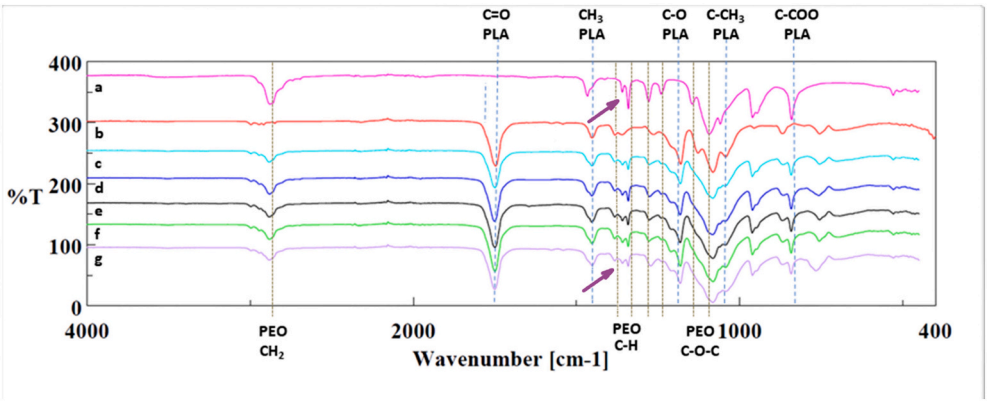

Fig. 1. FT-IR spectra of a) pure PEO, b) pure PLA and Samples (c) S-1; (d) S-2; e) S-3; f) S-4; g) S-5.

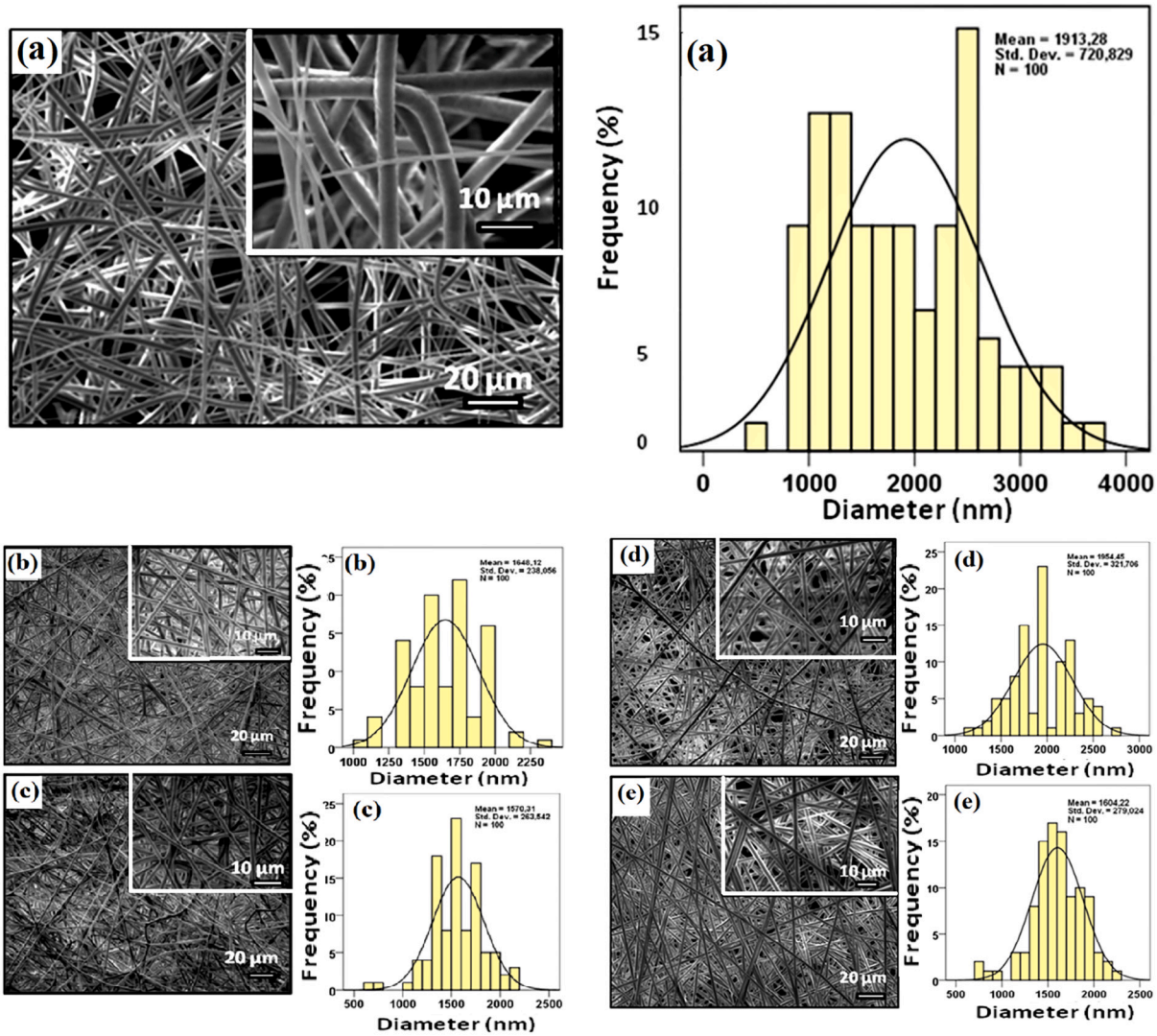

Fig. 2. SEM image of electrospun fibers and their diameter distributions. Samples a) S1; b) S2; c) S3; d) S4; e) S5.

have a lower average diameter and narrower size distribution compared to unfilled PLA/PEO fibers (Fig. 2). This was due to the interaction of the filler with the polymer matrix via hydrogen bonds. Additionally, Sample-S3 exhibited narrower size distribution and lower average fiber diameter (1570.31 nm) than the others.

3.4. Tensile properties

Highly crystalline polymers have relatively higher tensile strength and lower strain values. Thus, the electrospun fibers of such polymers tend to break spontaneously when they are exposed to external stress. It was reported that the tensile strength and elongation values of a pure PLA film were 35 MPa and 4 %, respectively [38]. However, while the tensile strength of PLA/PEO mixtures decreased with increasing PEO fraction, the elongation value increased due to the plasticizing effect of PEO, resulting in a more amorphous structure [38]. Thus, the blend films of PLA and PEO became more flexible. Nijenhius et al. studied the effect of PEO concentration on the mechanical properties of PLA/PEO blends. The mechanical properties were remarkably influenced by PEO content at over 20 % of PEO concentration, and the PLA/PEO blends became more flexible with a 500 % elongation at break [10]. In our case, the tensile strength and elongation values of the PLA/PEO electrospun fibers (sample S-1, PLA/PEO ratio 8/5, 38 % of PEO), were determined to be 0.21 MPa with 12.21 % elongation, which are considerably different from the literature values. This was due to the fact that the samples were in electrospun fiber mat form rather than the polymer film and had different compositions (Table 2). When 0.6 % of Mg—Al LDH nanoparticles were added into the PLA/PEO blend, no significant change in tensile strength and elongation were observed. However, the addition of 1.24 % Mg-Al LDH nanoparticles resulted in a remarkable increase in tensile strength and elongation (S-4 and S-5). This was probably due to the penetration of the nanoparticles into the polymer chains and connecting them through the hydrogen bonds between the hydrogen of –OH groups of Mg—Al LDH and the oxygen atoms of carbonyl and ether groups of PLA/PEO polymer matrix, which led to the improved mechanical properties. This interaction was supported by FTIR and DSC measurements as well.

3.5. Thermal Analysis

3.5.1. TGA

Thermal gravimetric analysis (TGA) is a helpful technique to determine the thermal behavior of polymeric materials as a function of temperature. Thus, the TGA curves of the unfilled and filled samples were recorded. Fig. 3a shows the weight loss curves of the pure polymers. PLA and PEO had a single-step weight-loss behavior. While the thermal decomposition of PLA started at 297 °C and ended at 382 °C, these temperatures were 347 °C and 429 °C for PEO, respectively. PEO

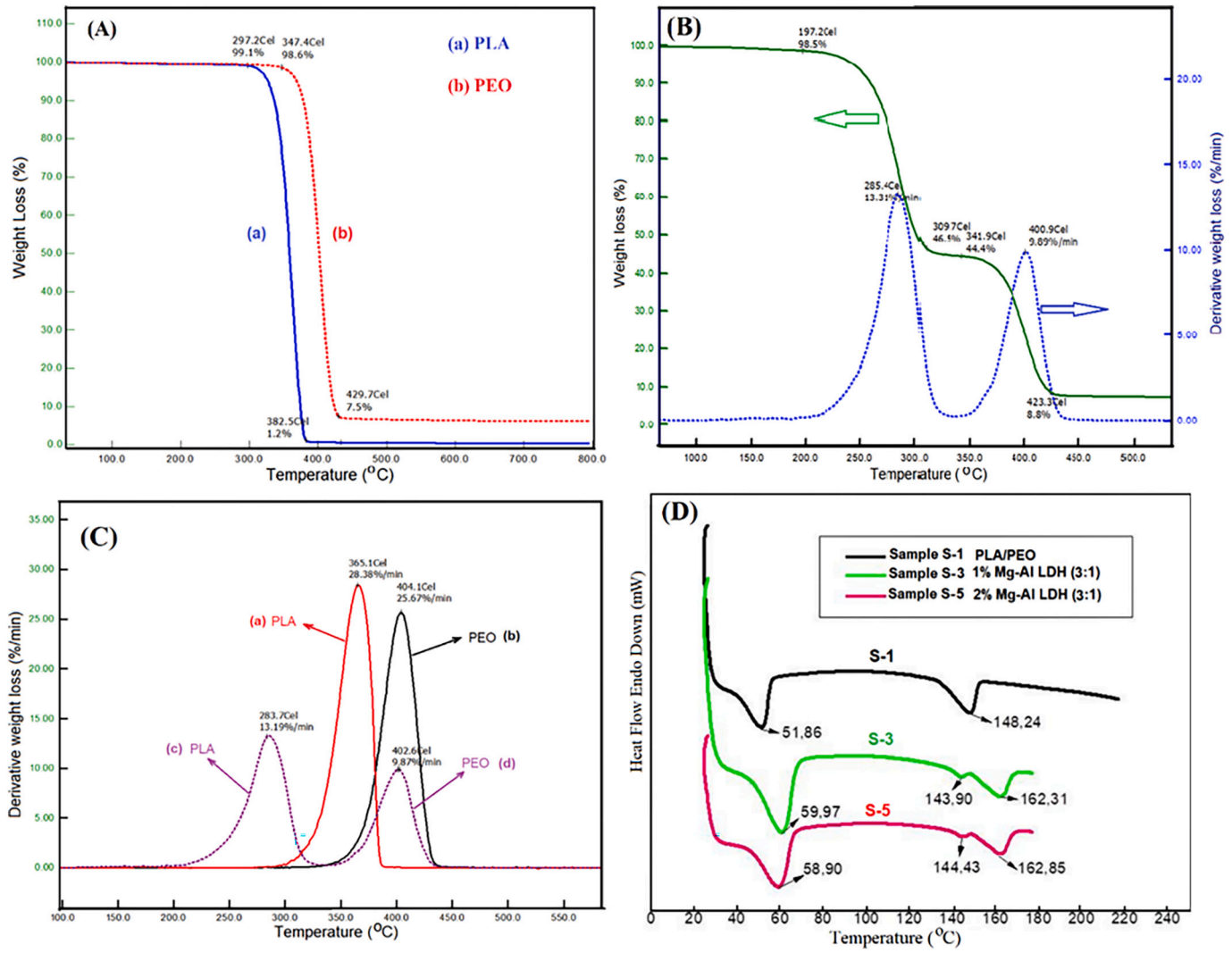

Fig. 3. (A) Weight-loss curves of PEO and PLA. (B) Weight-loss and derivative weight loss curves of Sample-S5 (Mg—Al LDH (3:1) 2 %). (C) Derivative weight-loss curves of Sample-S5, PLA and PEO. (D) DSC curves of Sample-S1, Sample-S3, and Sample-S5.

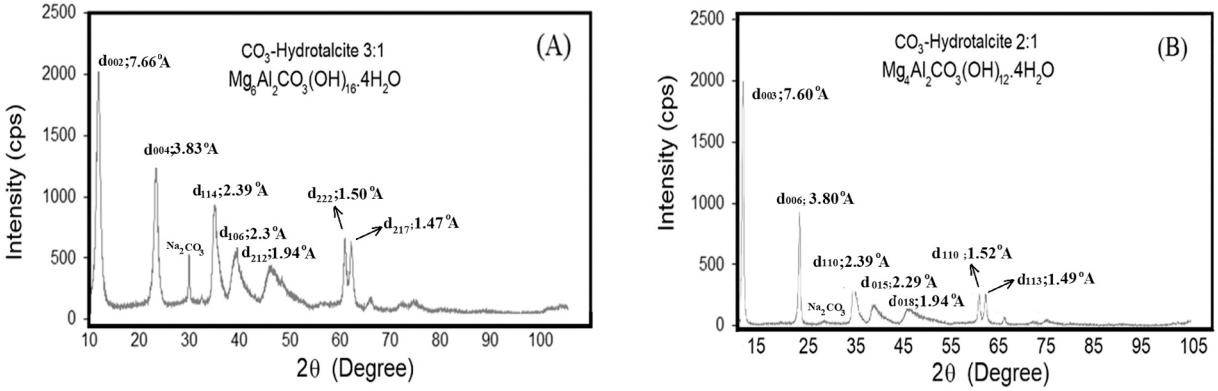

Fig. 4. XRD patterns of (A) Mg—Al LDH (3:1); (B) Mg—Al LDH (2:1).

had higher thermal stability than PLA. Fig. 3b shows TG and derivative TG (DTG) curves of sample S-5, containing 1.24 % Mg-Al LDH 3:1 (Table 2). As shown in this figure, sample S-5 displayed a two-step weight-loss process, i.e., first PLA and then PEO decompositions. Comparison of the thermal stabilities of unfilled PLA/PEO and sample S-5 indicated that, while there was no remarkable change in the decomposition temperature of PEO, PLA decomposition temperature decreased from 297 °C to 197 °C. This result is consistent with the previous findings of Demirkaya et al. [23]. In a separate study, Ray et al., reported that the lower thermal stability of PLA might be due to the presence of –OH groups of the homogeneously dispersed nano LDH filler in the PLA/PEO matrix, which may lead to a hydrolytic decomposition

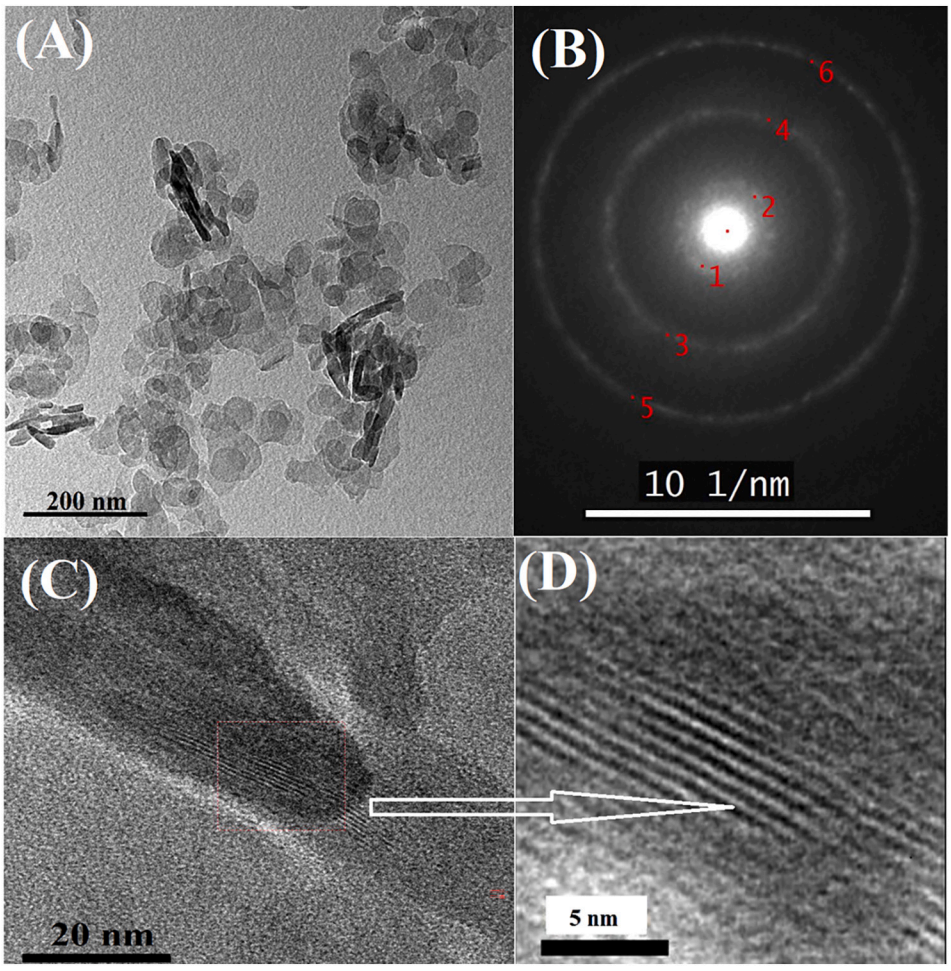

Fig. 5. TEM images and selected area pattern (SAED) of Mg—Al LDH (3:1) (A, C, D) and diffraction pattern (B).

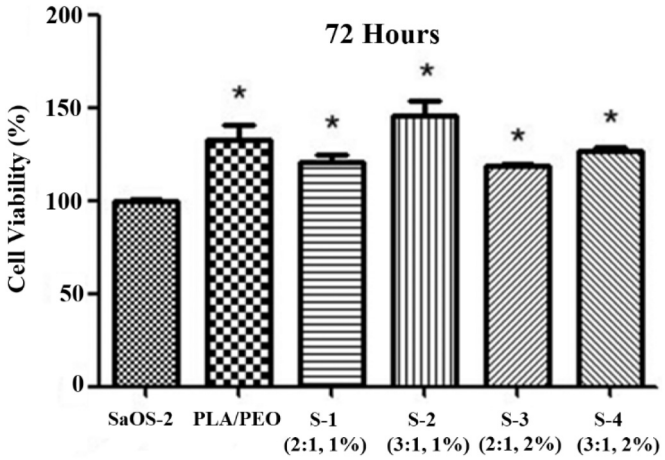

Fig. 6. SaOS-2 human bone osteosarcoma cell proliferation and viability on the composite electrospun fiber mats.

of the ester sites on the PLA chains [39,40]. Moreover, to elucidate the effect of the filler on the weight-loss rate of the samples, their derivative weight-loss curves (DTG) were recorded. It is well known that the DTG peak area and the corresponding peak temperature could be considered as a direct quantitative measure of the thermal stability of polymeric materials. Therefore, a comparison of the DTG peak temperatures of PLA/PEO fiber and the composite sample S-5 could be more informative to determine how Mg—Al LDH nanofiller affected the weight-loss rate and temperature of the components. As shown in Fig. 3c, although Mg—Al LDH (3:1) caused a profound decrease in the maximum weight-loss rate temperature of PLA, it had no remarkable effect on PEO. It is notable that, PLA/PEO blend had a slower weight-loss rate (as %/min) in the presence of Mg—Al LDH (3:1) than that of the unfilled form.

3.5.2. DSC

DSC can provide useful information regarding the melting behavior and morphological structure of the components in a polymer blend. This technique has been used extensively to estimate the compatibility of the ingredients in composite samples. The peak temperature and peak area of a DSC curve are characteristics of a pure sample. Regarding composite materials, the DSC technique provides quantitative information on the melting behavior and energetic interactions between ingredients. Melting temperatures of PEO and PLA in blend form (sample S-1) were found to be 51 °C and 148 °C, respectively (Fig. 3d) [12,28]. However, the melting temperatures of PEO and PLA in the composite matrix (samples S-3 and S-5) were observed nearly at 59 °C and 162 °C, respectively. Mg—Al LDH (3:1) considerably shifted the melting temperatures of PLA and PEO to higher temperatures. This finding was considered to be another evidence of the interactions between the filler and the polymer matrix, which means Mg—Al LDH nanoparticles affected the morphology of the polymer matrix.

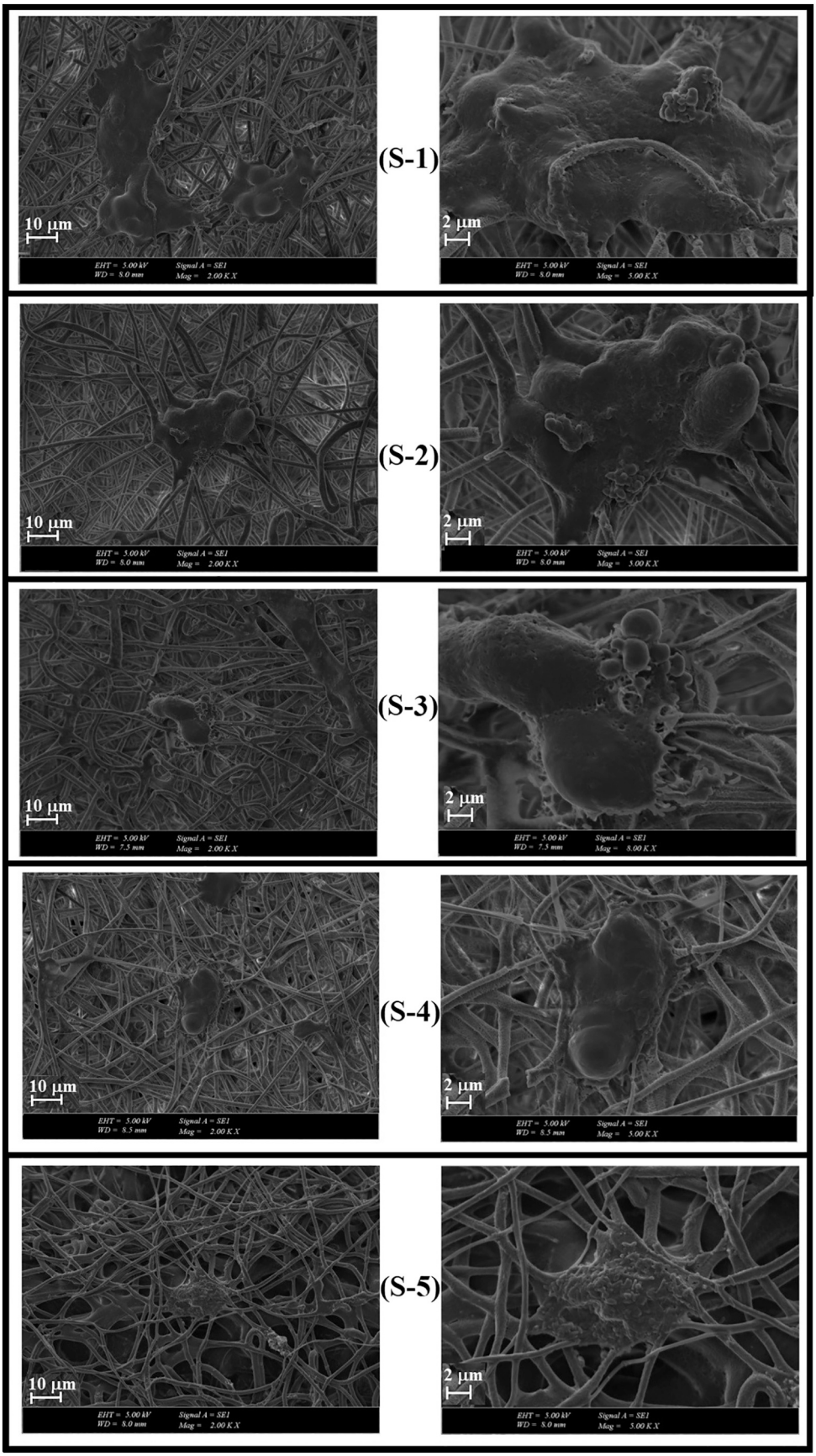

Fig. 7. SEM images of proliferated SaOS-2 human bone osteosarcoma cell at 2.0 K and 5.0 K magnification. Scale bars are 10 μm and 2 μm.

3.6. XRD and TEM

3.6.1. XRD

Detailed structural analysis of the Mg—Al LDH nanoparticles was conducted using X-ray diffraction spectroscopy (XRD) and transmission electron microscopy (TEM) techniques. Fig. 4 shows XRD patterns of Mg—Al LDH(3:1) and Mg—Al LDH (2:1) in the 2θ range of 5°-105°. Interlayer spacing of the LDH layers was calculated according to Bragg's equation. The XRD pattern of Mg—Al LDH (3:1) is presented in Fig. 4A. It is well known that XRD peak intensities depend on the number of planes diffracting the incoming X-ray quanta's at the same 2θ values. Thus, the interlayer distance of the hexagonal main plane of the sample at 2θ = 11.54° d(002) was calculated as 7.66 °A. Other XRD peaks and their interlayer distance are 2θ = 23.19° d(004), 3.83 Å; 2θ = 37.59° d (114), 2.39 Å; 2θ = 39.12° d(106), 2.30 Å; 2θ = 46.84° d(212), 1.94 Å; 2θ = 61.78° d(222), 1.50 Å and 2θ = 62.73° d(217), 1.48 Å. Fig. 4B represents the XRD peaks and the interlayer distance of hexagonal Mg—Al LDH (2:1). The main plane of the sample at 2θ = 11.62° was calculated as d(003), 7.60 Å. Other XRD peaks are 2θ = 23.38° d(006), 3.80 Å; 2θ = 37.45° d(110), 2.39 Å; 2θ = 39.35° d(015), 2.29 Å; 2θ = 46.81° d(018), 1.94 Å; 2θ = 60.59° d(110), 1.52 Å and 2θ = 62.00° d (113), 1.49 Å. The main 2θ values of the spectra were observed to be similar to those reported by Bernard et al. [41].

3.6.2. TEM

TEM micrographs and diffraction patterns were recorded to obtain information about the shape and size of crystalline particles and the average distance between crystal layers. Fig. 5 shows the TEM images at different magnifications and selected area diffraction pattern (SAED) of Mg—Al LDH (3:1). The particles are nearly round/hexagonal in shape and 50 nm in size (Fig. 5A). The diffraction planes (1,2), (3,4), (5,6) of the Mg—Al LDH (3:1) crystal belonging to the first, second, and third zones/circles in the pattern, corresponded to an average d spacings of 0.6561 nm, 0.2394 nm, 0.1499 nm, respectively (Fig. 5D). These results were found to be in good agreement with the interlayer spacing data obtained from the XRD measurements. The energy dispersive spectroscopy (EDS) analysis of the hydrotalcite nanostructure indicated that the Mg/Al ratio is nearly 3:1 ($Mg_{19.13}$:$Al_{7.05}$ mol/mol) similar to ($Mg_6Al_2CO_3(OH)16{\cdot}4H_2O$) phase. Detailed characterization data of the Mg/Al 3:1 and 2:1 nanoparticles including TEM images, SAED, and EDS analyses are given in the supplementary data.

3.7. Cytotoxicity study

MTT analysis was applied to determine the relative SaOS-2 cell viability measurement of the electrospun fiber mats. As shown in Fig. 6, cell viability was observed for 72 h on unfilled (S-1) and filled samples (S-2, S-3, S-4, and S-5), which indicated no cytotoxic effect compared to the control. Notably, the highest cell proliferation was obtained with sample S-2. Cell attachment on electrospun fiber mats is an essential issue in cell scaffolds and tissue engineering. In cell adhesion and proliferation, surface morphology, fiber diameter, and cell contact area are effective in mimicking extracellular matrix components. Cells behave on a surface through a different strategy. If they do not attach or spread on the fiber surface, they will probably undergo apoptosis and die. On the other hand, when a fiber surface supports the cell attachment, proliferation and differentiation are observed. After seeding on the electrospun fibers and then culturing for 24 h, the morphology of SaOS-2 cells on the electrospun fiber samples was examined by SEM analysis (Fig. 7). The electrospun fibers supported the attachment and proliferation of SaOS-2 cells, where cell clusters were formed. Thus, the biocompatibility tests demonstrated that the electrospun formulations had satisfactory cytocompatibility and were worth for biomedical applications and tissue engineering. Locilento et al. investigated the human foreskin fibroblast (HFF1) cells attachment on the grape extracted PLA/PEO electrospun fibers. PEO supported cell attachment and proliferation on the fiber surface [42].

4. Conclusion

Hydrotalcite like Mg—Al LDH nanoparticles were prepared and used as filler in PLA/PEO electrospun fibers. The nanoparticles had average 50 nm diameter and homogeneous dispersion. The interlayer distance of the hexagonal main plane of the crystal structure was not significantly affected by Mg:Al mole ratio. The Intermolecular interaction between the filler and the polymer matrix was evaluated through spectroscopic and thermal analyses of the electrospun fibers. It was concluded that intermolecular interaction provided improved mechanical properties without decrease in cytocompatibility, cell proliferation and differentiation on the fiber surface. With the non-toxicity nature of the LDH nanoparticles and their improving effect on the mechanical properties, the possibility of LDH filled PLA/PEO electrospun composite fiber mats for the preparation of biocompatible cell scaffolds is suggested.

Declaration of competing interest

The authors declare that they have no known competing financial interests or personal relationships that could have appeared to influence the work reported in this paper.

Appendix A. Supplementary data

Supplementary data to this article can be found online at https://doi.org/10.1016/j.ijbiomac.2022.07.055.

References

[1] C.-C. Chen, J.-Y. Chueh, H. Tseng, H.-M. Huang, S.-Y. Lee, Preparation and characterization of biodegradable PLApolymeric blends, Biomaterials 24 (2003) 1167–1173.
[2] E. Balla, V. Daniilidis, G. Karlioti, T. Kalamas, M. Stefanidou, N.D. Bikiaris, A. Vlachopoulos, I. Koumentakou, D.N. Bikiaris, Poly(lactic acid): a versatile biobased polymer for the future with multifunctional properties—from monomer synthesis, polymerization techniques and molecular weight increase to PLA applications, Polymers 13 (2021) 1822.
[3] G. Bang, S.W. Kim, Biodegradable poly(lactic acid)-based hybrid coating materials for food packaging films with gas barrier properties, J. Ind. Eng. Chem. 18 (2012) 1063–1068.
[4] B. Gupta, N. Revagade, J. Hilborn, Poly(lactic acid) fiber: an overview, Prog. Polym. Sci. 32 (2007) 455–482.
[5] H. Bi, T. Feng, B. Li, Y. Han, In vitro and in vivo comparison study of electrospun PLA and PLA/PVA/SA fiber membranes for wound healing, Polymers 12 (2020) 839.
[6] D. Cohn, H. Younes, Biodegradable PEOlPLA block copolymers, J. Biomed. Mater. Res. 22 (1988) 993–1009.
[7] O. Martin, L. Averous, Poly(lactic acid): plasticization and properties of biodegradable multiphase systems, Polymer 42 (2001) 6209–6219.
[8] M. Baiardo, G. Frisoni, M. Scandola, M. Rimelen, D. Lips, K. Ruffieux, E. Wintermantel, Thermal and mechanical properties of plasticized poly(L-lactic acid), J. Appl. Polym. Sci. 90 (2002) 1731–1738.
[9] Y. Eom, B. Choi, S. Park, A study on mechanical and thermal properties of PLA/PEO blends, J. Polym. Environ. 27 (2018) 256–262.
[10] A.J. Nijenhuis, E. Colstee, D.W. Grijpma, A.J. Pennings, High molecular weight poly(L-lactide) and poly(ethylene oxide) blends: thermal characterization and physical properties, Polymer 37 (26) (1996) 5849–5857.
[11] T. Caykara, S. Demirci, M.S. Eroglu, O. Guvenc, Poly(ethylene oxide) and its blends with sodium alginate, Polymer 46 (2005) 10750–10757.
[12] M. Sennaroglu Bostan, E. Cansever Mutlu, H. Kazak, S.S. Keskinc, E. Toksoy Oner, M.S. Eroglu, Comprehensive characterization of chitosan/PEO/levan ternary blend films, Carbohydr. Polym. 102 (2014) 993–1000.
[13] M.M. Amiji, Permeability and blood compatibility properties of chitosan-poly (&ylen& oxide) blend membranes for haemodialysis, Biomaterials 16 (1995) 593–599.
[14] C. Nakafuku, M. Sakoda, Melting and crystallization of poly(L-lactic acid) and poly (ethylene oxide) binary mixture, Polym. J. 25 (9) (1993) 909–917.
[15] M.-F. Chiang, M.-Z. Chu, T.-M. Wu, Effect of layered double hydroxides on the thermal degradation behavior of biodegradable poly(L-lactide) nanocomposites, Polym. Degrad. Stab. 96 (2011) 60–66.
[16] V.H. DeLeon, T.D. Nguyen, M. Nar, N.A. D'Souza, T.D. Golden, Polymer nanocomposites for improved drug delivery efficiency, Mater. Chem. Phys. 132 (2012) 409–415.

[17] Y. Kuang, L. Zhao, S. Zhang, F. Zhang, M. Dong, S. Xu, Morphologies, preparations and applications of layered double hydroxide micro-/nanostructures, Materials 3 (2010) 5220–5235.
[18] N. Zhao, S. Shi, G. Lu, M. Wei, Polylactide (PLA)/layered double hydroxides composite fibers by electrospinning method, J. Phys. Chem. Solids 69 (2008) 1564–1568.
[19] M. Chakraborty, S. Dasgupta, C. Soundrapandian, J. Chakraborty, S. Ghosh, S. M. Mitra, D. Basu, Methotrexate intercalated ZnAl-layered double hydroxide, J. Solid State Chem. 184 (2011) 2439–2445.
[20] J.B. Moreira, A.L.M. Terra, J.A.V. Costa, M.G. de Morais, Development of pH indicator from PLA/PEO ultrafine fibers containing pigment of microalgae origin, Int. J. Biol. Macromol. 118 (2018) 1855–1862.
[21] E. Yeniay, L. Öcal, E. Altun, B. Giray, F.N. Oktar, A.T. Inan, N. Ekren, O. Kilic, O. Gunduz, Nanofibrous wound dressing material by electrospinning method, Int. J. Polym. Mater. Polym. Biomater. 68 (2018) 11–18.
[22] N. Bhardwaj, S.C. Kundu, Electrospinning: a fascinating fiber fabrication technique, Biotechnol. Adv. 28 (2010) 325–347.
[23] Z.D. Demirkaya, B. Sengul, M.S. Eroglu, N. Dilsiz, Comprehensive characterization of polylactide-layered double hydroxides nanocomposites as packaging materials, J. Polym. Res. 22 (7) (2015) 1–13.
[24] Y.E. Miao, H. Zhu, D. Chen, R. Wang, W.W. Tjiu, T. Liu, Electrospun fibers of layered double hydroxide/biopolymer nanocomposites as effective drug delivery systems, Mater. Chem. Phys. 134 (2012) 623–630.
[25] P. Mróz, S. Białas, M. Muchaa, H. Kaczmarek, Thermogravimetric and DSC testing of poly(lactic acid) nanocomposites, Thermochim. Acta 573 (2013) 186–192.
[26] Y. Hu, M. Rogunova, V. Topolkaraev, A. Hiltner, E. Baer, Aging of poly(lactide)/poly(ethylene glycol) blends. Part 1. Poly(lactide) with low stereoregularity, Polymer 44 (2003) 5701–5710.
[27] G. Sun, L.-T. Weng, J.M. Schultz, C.-M. Chan, Formation of banded and non-banded poly(L-lactic acid) spherulites during crystallization of films of poly(L-lactic acid)/poly(ethylene oxide) blends, Polymer 55 (2014) 1829–1836.
[28] Y. Fang, Study of the development of elastomer nanoparticles and their application as reinforcing agents for poly(lactic acid), in: Food and Nutrition, Université de Lorraine, 2012.
[29] T. Mosmann, Rapid colorimetric assay for cellular growth and survival: application to proliferation and cytotoxicity assays, J.Immunol.Methods 65 (1983) 55–63.
[30] P. Gupta, C. Elkins, T.E. Long, G.L. Wilkes, Electrospinning of linear homopolymers of poly(methyl methacrylate): exploring relationships between fiber formation, viscosity, molecular weight and concentration in a good solvent, Polymer 46 (2005) 4799–4810.
[31] A. Luzio, E.V. Canesi, C. Bertarelli, M. Caironi, Electrospun polymer fibers for electronic applications, Materials 7 (2014) 906–947.
[32] M.M. Demir, I. Yilgor, E. Yilgor, B. Erman, Electrospinning of polyurethane fibers, Polymer 43 (2002) 3303–3309.
[33] K.H. Lee, H.Y. Kim, Y.M. La, D.R. Lee, N.H. Sung, Influence of a mixing solvent with tetrahydrofuran and N, N-dimethylformamide on electrospun poly(vinyl chloride) nonwoven mats, J. Polym. Sci. B Polym. Phys. 40 (2002) 2259–2268.
[34] M. Zamani, M. Morshed, J. Varshosaz, M. Jannesari, Controlled release of metronidazole benzoate from poly e-caprolactone electrospun nanofibers for periodontal diseases, Eur. J. Pharm. Biopharm. 75 (2010) 179–185.
[35] M.O. Aydogdu, J. Chou, E. Altun, N. Ekren, S. Cakmak, M. Eroglu, A.A. Osman, O. Kutlu, E. Toksoy Oner, G. Avsar, F.N. Oktar, I. Yilmaz, O. Gunduz, Production of the biomimetic small diameter blood vessels for cardiovascular tissue engineering, Int.J.Polym.Mater.Polym.Biomater. 68 (5) (2018) 243–255.
[36] R. Konwarh, N. Karak, M. Misra, Electrospun cellulose acetate nanofibers: the present status and gamut of biotechnological applications, Biotechnol. Adv. 31 (2013) 421–437.
[37] I. Pucić, T. Jurkin, FTIR assessment of poly(ethylene oxide) irradiated in solid state, melt and aqeuous solution, Radiat. Phys. Chem. 81 (2012) 1426–1429.
[38] M. Ho, K. Lau, H. Wang, D. Hui, Improvement on the properties of polylactic acid (PLA) using bamboo charcoal particles, Compos.Part B 81 (2015) 14–25.
[39] S. Sinha Ray, M. Okamoto, Polymer/layered silicate nanocomposites: a review from preparation to processing, Prog. Polym. Sci. 28 (2003) 1539–1641.
[40] S. Sinha Ray, K. Yamada, M. Okamoto, K. Ueda, New polylactide-layered silicate nanocomposites. 2. Concurrent improvements of material properties, biodegradability and melt rheology, Polymer 44 (2003) 857–866.
[41] E. Bernard, W.J. Zucha, B. Lothenbach, U. Mader, Stability of hydrotalcite (Mg-Al layered double hydroxide) in presence of different anions, Cem. Concr. Res. 152 (2022), 106674.
[42] D.A. Locilento, L.A. Mercante, R.S. Andre, L.H.C. Mattoso, G.L.F. Luna, P. Brassolatti, F.de F. Anibal, D.S. Correa, Biocompatible and biodegradable electrospun nanofibrous membranes loaded with grape seed extract for wound dressing application, Hindawi J. Nanomater. 11 (2019), 2472964.